Regular Article

IMMUNOBIOLOGY

# Antibody Fc engineering improves frequency and promotes kinetic boosting of serial killing mediated by NK cells

Gabrielle Romain,[1] Vladimir Senyukov,[2] Nicolas Rey-Villamizar,[3] Amine Merouane,[3] William Kelton,[4] Ivan Liadi,[1] Ankit Mahendra,[1] Wissam Charab,[4] George Georgiou,[4] Badrinath Roysam,[3] Dean A. Lee,[2] and Navin Varadarajan[1]

[1]Department of Chemical and Biomolecular Engineering, University of Houston, Houston, TX; [2]Division of Pediatrics, University of Texas M.D. Anderson Cancer Center, Houston, TX; [3]Department of Electrical Engineering, University of Houston, Houston, TX; and [4]Department of Chemical Engineering, Institute for Cell and Molecular Biology, University of Texas, Austin, TX

## Key Points

- Fc-engineered mAb promotes NK cell ADCC via better activation, serial killing, and kinetic boosting at higher target cell densities.
- Enhanced target killing also increased frequency of NK cell apoptosis, but this effect is donor-dependent.

**The efficacy of most therapeutic monoclonal antibodies (mAbs) targeting tumor antigens results primarily from their ability to elicit potent cytotoxicity through effector-mediated functions. We have engineered the fragment crystallizable (Fc) region of the immunoglobulin G (IgG) mAb, HuM195, targeting the leukemic antigen CD33, by introducing the triple mutation Ser293Asp/Ala330Leu/Ile332Glu (DLE), and developed Time-lapse Imaging Microscopy in Nanowell Grids to analyze antibody-dependent cell-mediated cytotoxicity kinetics of thousands of individual natural killer (NK) cells and mAb-coated target cells. We demonstrate that the DLE-HuM195 antibody increases both the quality and the quantity of NK cell-mediated antibody-dependent cytotoxicity by endowing more NK cells to participate in cytotoxicity via accrued CD16-mediated signaling and by increasing serial killing of target cells. NK cells encountering targets coated with DLE-HuM195 induce rapid target cell apoptosis by promoting simultaneous conjugates to multiple target cells and induce apoptosis in twice the number of target cells within the same period as the wild-type mAb. Enhanced target killing was also associated with increased frequency of NK cells undergoing apoptosis, but this effect was donor-dependent. Antibody-based therapies targeting tumor antigens will benefit from a better understanding of cell-mediated tumor elimination, and our work opens further opportunities for the therapeutic targeting of CD33 in the treatment of acute myeloid leukemia. (*Blood*. 2014;124(22):3241-3249)**

## Introduction

Therapeutic monoclonal antibodies (mAbs) elicit functional responses through many different mechanisms, including antibody-dependent cell-mediated cytotoxicity (ADCC), complement dependent cytotoxicity, antibody-dependent cell-mediated phagocytosis (ADCP), and direct induction of apoptosis in tumor cells.[1] By using the principles of glycoengineering and mutagenesis, Fc variants have been isolated that show either increased affinity for the activating receptors or altered selectivity for the activating/inhibitory receptors.[2-4] Preliminary clinical data with such antibodies Fc-engineered to improve the ADCC/ADCP potential and targeting CD19, CD20, Her2, or CD40 have shown reasonable promise in improving the therapeutic potential of mAb.[5-8] Natural killer (NK) cells occupy a pivotal role in immunity: not only can they exert direct cytotoxicity toward infected or tumor cells but they also participate in shaping the adaptive response.[9,10] In the context of mAb treatment, NK cells are unique in that they express only the low-affinity activating FcγR CD16 (FcγRIIIa), and no inhibitory antibody receptors, underscoring a significant role in ADCC.[11-13] Several studies using mouse tumor models have established a link between activating Fc receptors and the efficacy of mAb therapy.[14,15] Furthermore, as CD16 is polymorphic in humans, it has been demonstrated previously that immune cells that harbor the CD16-158V allotype exhibit better binding to human immunoglobulin G1 (IgG1), which in turn leads to more efficient ADCC/ADCP in vitro and to better clinical outcomes.[16-19]

Acute myeloid leukemia (AML) is the most common acute leukemia affecting adults and is responsible for more than 10 000 deaths annually in the United States. Therapeutic strategies to treat AML with mAbs have predominantly targeted the sialic acid-binding sialoadhesin receptor 3 (CD33), which is expressed in more than 85% of leukemic cells, including leukemic stem cells.[20] Gemtuzumab ozogamicin, an immunoconjugate between the humanized M195 antibody and the DNA-damaging toxin calicheamicin, was granted expedited approval by the US Food and Drug Administration in 2000 on the basis of promising phase 2 data.[21] In 2010, however, gemtuzumab ozogamicin was withdrawn because of toxicities that affected the risk–benefit ratio. Recent clinical data showing efficacy in AML patients have challenged this withdrawal.[21,22] The unconjugated anti-CD33 antibody, M195, and its humanized version,

Submitted April 9, 2014; accepted August 27, 2014. Prepublished online as *Blood* First Edition paper, September 16, 2014; DOI 10.1182/blood-2014-04-569061.

G.R. and V.S. contributed equally to this study.

The online version of this article contains a data supplement.

There is an Inside *Blood* Commentary on this article in this issue.

The publication costs of this article were defrayed in part by page charge payment. Therefore, and solely to indicate this fact, this article is hereby marked "advertisement" in accordance with 18 USC section 1734.

HuM195 (lintuzumab),[23] have only shown limited benefit in clinical trials, but mechanistic studies have demonstrated a significant role for effector functionality (ADCC and ADCP), suggesting that Fc engineering can improve clinical efficacy.[24]

Although Fc engineering can increase molecular affinity toward CD16, the mechanistic basis of the improved affinity resulting in better ADCC by NK cells is not well established. In vitro dynamic imaging systems are particularly suited for studying the dynamics of cell–cell interactions in a defined environment but have been typically limited in throughput and in monitoring effector fate.[25-28] We engineered the Fc region of the anti-CD33 mAb HuM195 by introducing the triple mutation S293D/A330L/I322E (DLE) and developed Time-lapse Imaging Microscopy in Nanowell Grids (TIMING) to analyze ADCC kinetics of thousands of individual NK cells incubated with mAb-coated target cells. We demonstrate that mAb Fc engineering promotes superior activation of NK cells and improves both amplitude and kinetics of NK cell-mediated ADCC. Furthermore, NK cell-mediated ADCC can induce activation-induced cell death (AICD) in effector cells, although this was subject to donor heterogeneity. These results can shed light on both the mechanism underlying improved ADCC and the decreased frequency of NK cells in peripheral circulation seen on treatment with Fc-engineered antibodies, and can also support the reevaluation of anti-CD33 antibodies.

## Methods

### Human subjects' statement

All protocols listed in this study were reviewed and approved by the institutional review boards at the University of Houston and the University of Texas M.D. Anderson Cancer Center.

### Statistical analysis

The tests used to determine the *P* values are listed in supplemental Table 1 available on the *Blood* Web site and are indexed in the main manuscript, using subscripts.

### Antibody engineering and expression

The variable domains of light- and heavy-chain genes of HuM195 were constructed by using recursive polymerase chain reaction and were cloned into expression plasmids, as described previously.[29] Mutations were introduced into the heavy chain using QuikChange mutagenesis techniques (Stratagene). Light- and heavy-chain plasmids were prepared by using a Biomek FX (Beckman Coulter) and cotransfected into 293T cells. Supernatants were harvested and antibodies were purified by using protein A affinity chromatography (Pierce). The affinity of wild-type (wt)-HuM195 and DLE-HuM195 for CD16 or CD33 was tested using sandwich enzyme-linked immunosorbent assay (ELISA).

### Fabrication of nanowell array and end-point cytotoxicity assay

Nanowell array fabrication and single-cell level cytotoxicity assay were performed as described previously.[27] Briefly, $CD33^+$EL4 (targets) and NK (effectors) cells were labeled for 5 minutes with 1 μM red PKH26 and green PKH67 (Sigma-Aldrich), respectively. The targets were subsequently incubated with 1 μg/mL mAb at 4°C for 20 minutes and were washed to remove excess mAb. Effectors and targets were loaded sequentially onto nanowell arrays at a concentration of $10^6$ cells/mL and the entire chip was incubated in complete medium containing 1/60th AnnexinV-AlexaFluor-647 (Life Technologies). Images were acquired on an AxioObserver (Carl Zeiss) fitted with a Hamamatsu electron multiplying charge coupled device camera using a 10 × 0.3 NA objective. Automated image acquisition of the array was performed at 0 and 6 hours. Detailed experimental design and background subtraction are described in supplemental Figure 3.

### TIMING assays

Nanowell arrays approximately one-third the original size were fixed onto a 60-mm Petri dish and loaded with labeled and mAb-pretreated cells as in the endpoint assay. The chip was immersed in phenol red-free complete medium and placed in a stage prepared for live cell imaging. Images were taken using a 20 × 0.45 NA objective for 12 to 16 hours at intervals of 7 to 10 minutes (supplemental Figure 5).

The supplemental Methods contains an extended description of cell lines, NK cell expansion protocols and phenotyping, image segmentation and tracking, and measurement of Zeta-chain-associated protein kinase 70 (ZAP-70) phosphorylation.

## Results

### Quantifying NK cell-mediated ADCC and AICD at the single-cell level

Starting with reported variable chain fragment sequences of the anti-CD33 antibody HuM195 as the template and the wt human IgG1 Fc, site-directed mutagenesis was employed to engineer the DLE mutations into the Fc region.[30] As demonstrated recently, the DLE mutations increase the affinity of the Fc toward both CD16-158 allotypes.[31] Sandwich ELISA confirmed that DLE-HuM195 had increased affinity toward CD16 with no change in antigen-binding affinity (Figure 1A-B).

To compare the effector functions of DLE-HuM195 with that of wt-HuM195, we first tested their potency to induce ADCC in 3 AML human cell lines expressing varying amounts of CD33: MV4:11, MOLM13, and HL60.[32] For all 3 lines tested, NK cell-mediated lysis was more pronounced on target cells that were precoated with DLE-HuM195 than on those precoated with wt-HuM195 (Figure 1C-E $P_1$, $P_2$, and $P_3$ values $< .0001$; details of tests listed in supplemental Table 1). As evidenced from the "no mAb" control, and because these tumor cell lines express additional ligands that facilitate NK cell-mediated cytotoxicity, we used the EL4 cell line (resistant to NK cell-mediated direct killing) expressing human CD33 (supplemental Figure 1A) to clearly define the contribution of mAb-derived ADCC.[33] As effector cells, we used human NK cells expanded ex vivo by following a protocol we have recently described for the generation of clinical-grade NK cells used in adoptive cell therapy (supplemental Figure 1B).[34,35] As expected, comparisons of the cumulative responses as measured by the calcein-AM release assay,[35] showed that NK cell-mediated lysis was more pronounced on $CD33^+$EL4 target cells that were precoated with DLE-HuM195 (hereafter referred to as DLE-Targets) than on wt-Targets, both at varying concentrations of mAbs (Figure 1F, at 1 ng/mL, $P_4 = .01$; and 10-$10^3$ ng/mL, $P_4 < .001$) and at different E:T ratios (Figure 1G; 1.3- to 2-9 fold increase with a more marked effect at lower E:T ratio; $P_5 < .0001$). The NK cell cytotoxicity was even more markedly increased with DLE-Targets in comparison with wt-Targets when the antibodies were present in solution for the duration of the assay (Figure 1H; 8-28 fold increase; $P_6 < .0001$). This confirmed that the continuous presence of mAb does not inhibit the cytotoxicity of NK cells. We also excluded any direct cytotoxic effect of the mAbs by incubating the $CD33^+$EL4 targets with the same mAbs (1 μg/mL), but without adding NK cells (supplemental Figure 2A), as well as by incubating NK cells with mAb only, without targets (supplemental Figure 2B).

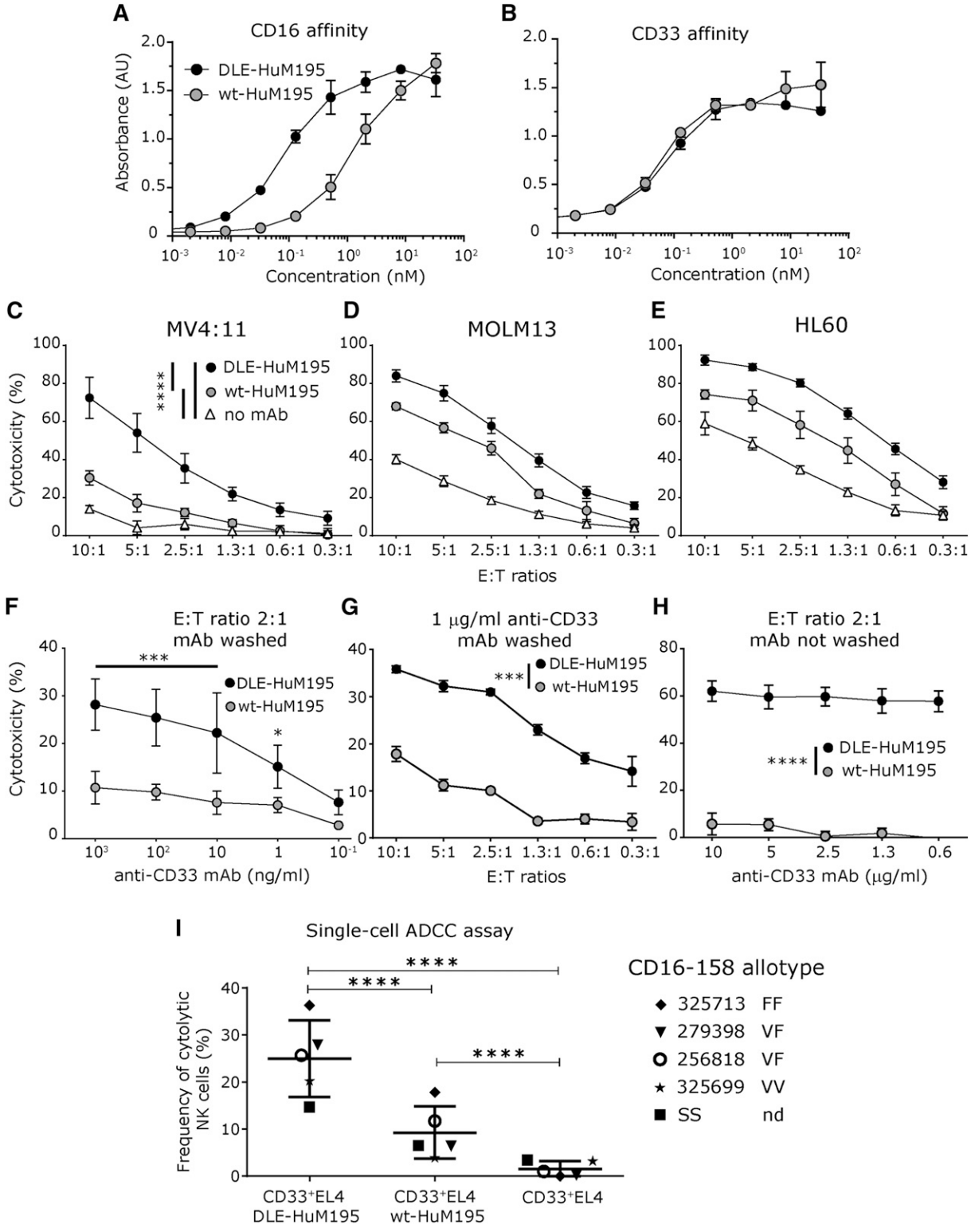


**Figure 1. Engineering the triple mutation, DLE, into the CH2 domain of the anti-CD33 antibody improves NK cell-mediated ADCC.** (A-B) Sandwich ELISA confirmed that the affinity of Fc-engineered DLE-HuM195 for CD16 is increased, relative to wt-HuM195, with no change in antigen affinity (CD33). (C-E) Population-level calcein AM release assays profiling cytotoxicity of ex vivo NK cells against mAb-precoated AML cell lines at varying E:T ratios and a fixed concentration of mAb (1 μg/ml). N = 3 donors, run in triplicate, for 6 hours. (F-H) Population-level calcein AM release assay run against $CD33^+$EL4 target cells incubated with mAb. NK cell-mediated lysis when targets were precoated with mAb (excess mAb is washed away after preincubation) at (F) a fixed E:T ratio, but varying mAb concentration, and (G) fixed mAb concentration but varying E:T ratios. (H) NK cell-mediated target lysis when mAb is present in solution for the duration of the assay. Frequencies are reported with background correction (values obtained without mAb). (I) Single-cell endpoint cytotoxicity assay. Labeled $CD33^+$EL4 target cells were precoated with mAb (1 μg/mL) and incubated on a nanowell array with labeled, expanded NK cells as effectors for 6 hours, and ADCC was determined as described in supplemental Figure 3 (E:T ratio, 1:1-3) (at least 2676 events were analyzed for each donor and mAb condition was tested). Of note, these values represent the background-corrected frequencies of cytolytic NK cells, which are obtained as described in supplemental Figure 3. When available, CD16-158 allotype is annotated near the donor identifying number (F, phenylalanine; V, valine). All data are shown as mean ± SD, and stars represent *P* values calculated as detailed in supplemental Table 1 ($P_1$-$P_7$). nd, not determined.

To quantify the frequency of cytotoxic NK cells, we set up a single-cell assay with appropriate controls (supplemental Figure 3), as described previously.[27] Fluorescently labeled annexin V was used to detect early apoptosis, and time-lapse microscopy using annexin V and Sytox (DNA dye) costaining confirmed that monitoring annexin V staining was sufficient to track eventual cell death (supplemental Video 1). Within nanowells containing a single NK cell and 1 to 3 targets, after 6 hours, 25% ± 8% (mean ± standard deviation [SD]; n = 5 donors) of NK cells induced apoptosis of DLE-Targets (Figure 1I). In comparison, only 9% ± 6% of NK cells induced apoptosis of wt-Targets, indicating a significant antibody-dependent effect in cytotoxicity at the single-cell level ($P_7 < .0001$). Under identical conditions, the frequency of NK cells that induced target apoptosis in the absence of antibody was negligible (2% ± 2%), confirming that cell cytotoxicity was dependent on preincubation with the antibody. Consistent with published results,[31] there was no correlation between CD16-158 allotype and the frequency of cytotoxic NK cells (Figure 1I). These results confirmed that the Fc-engineered DLE-HuM195 potentiated cytotoxicity of larger amplitude and higher frequencies of NK cells.

Unlike ADCC, which was uniformly improved across all NK cell samples tested, the frequency of cytotoxic NK cells undergoing AICD (supplemental Video 2) was heterogeneous: in 3 of 5 samples, frequency of NK cell AICD was a mean of 37% (range: 27-42%) when interacting with DLE-Targets, and a mean of 19% (range: 12-26%) when incubated with wt-Targets (supplemental Figure 4A; $P_8 < .01$). In contrast, with the other 2 samples, AICD frequency was not affected by the mAb pretreatment (supplemental Figure 4B; DLE-Targets, mean, 19% [range: 19-20%]; and wt-Targets, mean, 19% [range: 18-20%]; $P_9 > .05$). Taken together, these data suggest the DLE-engineered mAb can induce donor-specific antibody-dependent increases in AICD.

### TIMING to quantify the dynamic interactions between NK cells and target cells

To gain mechanistic insight into the interactions of NK cells and antibody-coated target cells, we measured in vitro the kinetics of their interactions, using TIMING (supplemental Figure 5). Individual NK cells derived from 3 separate donors with varying frequencies of ADCC, as determined by the end-point single-cell assay (Figure 1I and supplemental Table 2), were co-incubated with $CD33^+$EL4 target cells (1-3 cells) coated with either mAb and imaged by TIMING. To facilitate comparison with NK cell activation through natural cytotoxicity receptors or NK group 2, member D, parallel experiments were set up with the human HLA-deficient leukemic cell line K562 as target cells. Subsequent to automated image processing and segmentation, across these 3 samples, a total of 1233 (DLE-Targets), 1345 (wt-Targets), and 692 (K562 target cells) nanowells were identified as containing an E:T ratio of 1:1. As anticipated, the increased affinity of DLE-HuM195 for CD16 promoted longer contact durations between NK cells and antibody-coated targets ($P_{10} = .008$, supplemental Figure 6). At an E:T ratio of 1:1, a mean of 87% (range: 82-92%) of cytotoxic NK cells had an $n_{Conjugate}$, the number of unique conjugations (periods of continuous contact > 7 minutes), of 1 before killing DLE-Target; in comparison, a mean of 73% (range: 65-79%) of NK cells had an $n_{Conjugate}$ of 1 before being able to kill wt-Targets ($P_{11} < .0001$; Figure 2A).

Second, subsequent to at least 1 conjugation, a mean of 58% (range: 34-74%) of NK cells induced apoptosis of DLE-Targets, whereas only a mean of 33% (range: 9-47%) of NK cells induced apoptosis of wt-Targets ($P_{12} < .0001$; Figure 2B).

Third, $t_{Seek,}$ the time taken to establish the first conjugate (85 ± 6 minutes for DLE-Targets vs 83 ± 9 minutes for wt-Targets [mean ± standard error of the mean (SEM)]; Figure 2C), or $t_{Contact,}$ the total cumulative contact duration before tumor cell apoptosis (78 ± 4 minutes for DLE-Targets vs 93 ± 6 minutes for wt-Targets; Figure 2D), for NK cell-mediated ADCC was not different between the mAb treatments ($P_{13}$ and $P_{14}$). The major difference between both mAbs in inducing NK cell-mediated cytolysis was seen in the kinetics of target apoptosis: $t_{Death,}$ the time to induce target cell apoptosis from first contact, of DLE-Targets was 91 ± 5 minutes in comparison with a $t_{Death}$ for wt-Targets of 164 ± 11 minutes ($P_{15} < .0001$) (Figure 2E). Taken together, these kinetic data establish that compared with wt-HuM195, DLE-HuM195 increases the efficiency of target death by decreasing the time to target apoptosis, demonstrating that the increased molecular affinity for CD16 translates to more efficient contact, and enables faster cytotoxicity. In addition, curve-fitting the $t_{Contact}$ and $t_{Death}$ demonstrated that for both mAb treatments, a 2-phase decay model was appropriate (supplemental Table 3), suggesting that either different modes of killing (fast vs slow kinetics) or NK cell heterogeneity in cytotoxicity efficiency was present.

In comparison, for individual NK cells involved in the natural killing of single K562 cells, $t_{Seek}$ was 74 ± 8 minutes, $t_{Contact}$ was 119 ± 8 minutes, and $t_{Death}$ was 139 ± 11 minutes (Figure 2C-E). Thus, in comparison with natural killing, and despite similar $t_{Seek}$ ($P_{13} = .7$), DLE-HuM195 decreased the cumulative time of contact ($t_{Contact}$) and the overall time before target apoptosis ($t_{Death}$; $P_{16}$ and $P_{17}$ both < .0001).

To assess the effect of adhesion to target cells on the motility of the NK cells, their average displacement within nanowells (during each 7-minute timeframe), $d_{well}$, was computed in 3 phases: before, during, and after conjugation. Unlike their interaction with wt-Targets, individual NK cells interacting with single DLE-Targets showed, on conjugation, a significant decrease in motility (6.2 ± 0.3 μm vs 4.4 ± 0.2 μm [mean ± SEM]; $P_{18} < .0001$; Figure 2F) and polarization (eccentricity, 0.66 ± 0.01 vs 0.56 ± 0.01 μm; $P_{19} < .0001$; supplemental Figure 7). Similarly, on conjugation with K562 cells, single NK cells decreased their motility (5.7 ± 0.4 μm vs 4.0 ± 0.4 μm; $P_{20} < .0001$) and polarization (0.65 ± 0.02 vs 0.58 ± 0.02 μm; $P_{21} = .01$). These data suggest that individual NK cells encountering single DLE-Targets underwent efficient arrest, enabling a subsequent lytic hit.

### DLE-HuM195 promotes serial killing by individual NK cells via kinetic boosting

Because DLE-HuM195 significantly increased NK cell-mediated ADCC, we next investigated whether enhanced CD16 ligation would translate into increased serial killing by individual NK cells. Across 5 donors, within 6 hours, overall frequency of serial killing was higher with DLE-Targets (19% ± 8%, mean ± SD) compared with wt-Targets (5% ± 2%; $P_{22} < .0001$) (Figure 3A). Specifically, at an E:T ratio of 1:2 (supplemental Figure 8), 17% ± 7% of NK cells induced apoptosis of both DLE-Targets compared with 4% ± 1% with wt-Targets (Figure 3B; $P_{23} < .0001$). At an E:T ratio of 1:3, 14% ± 10% of NK cells induced apoptosis of all 3 separate DLE-Targets, which was significantly higher than individual NK cells inducing apoptosis of all 3 wt-Targets (2% ± 1%; $P_{24} = .03$). The probability of at least 1 killing event significantly increased with the number of targets in wells, regardless of the antibody variant tested (Figure 3B and supplemental Table 4), which can be attributed to a higher probability of encounter when

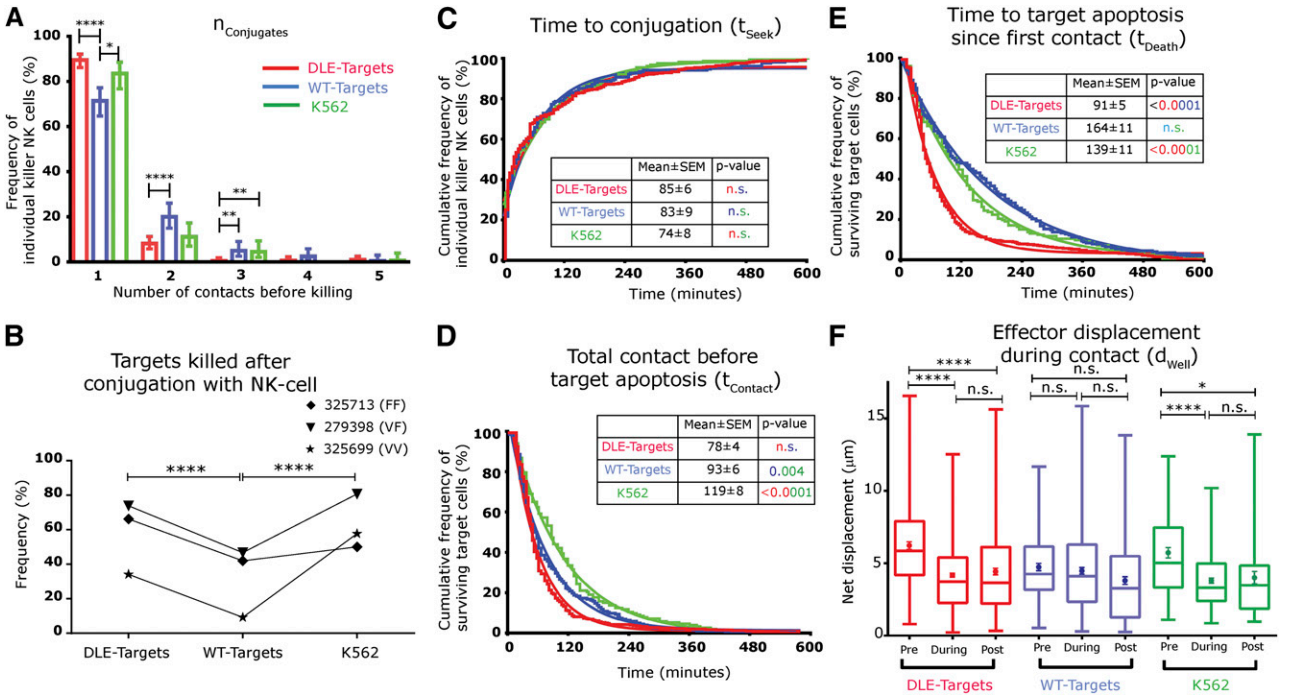


**Figure 2. DLE-HuM195 improves kinetic efficiency of NK cell-mediated ADCC, as uncovered by TIMING.** (A) Frequency distribution of number of conjugations preceding target cell apoptosis events, $n_{conjugates}$ (bars represent 95% confidence interval limits; stars represent statistical significance after Fisher exact test). (B) Frequency of NK cell target cell conjugates that subsequently lead to target cell apoptosis, regardless of the number of conjugates. Kaplan Meier curves (jagged lines) of (C) time taken to establish conjugates, $t_{Seek}$; (D) total contact duration before tumor cell apoptosis, $t_{Contact}$; (E) and time to induce target-apoptosis since first contact, $t_{Death}$, with each event being a single cytotoxic NK cell. Color coding of the *P* values is designed to reflect the groups being compared. (F) Effector motility, $d_{Well}$, during the different phases of target conjugation: before, during, and after. Data are represented in the box and whiskers plot (minimum, 25th percentile, median, 75th percentile, maximum) and mean ± SEM are shown (full circles and bars). The best fit data was obtained using curve fitting either 1-phase or 2-phase association/decay. The parameters obtained from the curve fit (smooth lines) are shown in supplemental Table 3. All data represented in this figure are derived from cytotoxic NK cells incubated at an E:T of 1:1. These data are derived from 1233 nanowells containing DLE-Targets, 1345 wt-Targets, and 692 K562 target cells. *P* values (eg, $P_{11}$-$P_{20}$) were calculated for each panel, as listed in supplemental Table 1.

more targets are present and/or to a higher probability of lysis when more targets are contacted (supplemental Table 5).

As described earlier, TIMING was employed to gain mechanistic insight into behavioral differences of NK cells in their interaction with target cells coated with either mAb. As anticipated by the higher tumor cell density (2-4 targets), the $t_{Seek}$ to conjugate to the first target was shorter in comparison with individual NK cells encountering single targets, both with wt-Targets (32 ± 4 minutes; $P_{25} = .03$) and DLE-targets (29 ± 6 minutes [mean ± SEM]; $P_{26} < .0001$) (Figure 4A). Striking differences were observed when comparing the kinetic efficiency of NK cells participating in serial killing of DLE-Targets (supplemental Video 3) and wt-Targets (supplemental Video 4). Both $t_{Contact}$ (48 ± 5 minutes for DLE-HuM195 vs 100 ± 9 minutes for wt-HuM195; $P_{27} < .0001$) and $t_{Death}$ of the first target

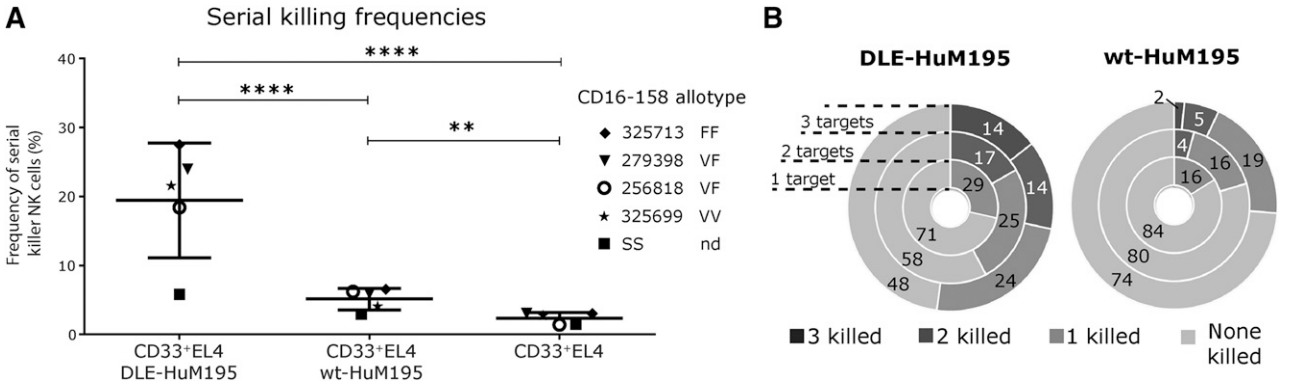


**Figure 3. DLE-HuM195 increases the frequency of NK cell-mediated serial killing.** (A) Overall serial killing frequencies (ability to kill at least 2 targets) of NK cells, as determined by the 6-hour endpoint single-cell assay (E:T ratio, 1:2-3) (at least 236 events were analyzed for each donor and mAb condition tested). These values represent the frequencies of serial killer NK cells as a percentage of all cytolytic NK cells incubated with 2-4 target cells. CD16-158 allotype is annotated near the donor identifying number. (B) Donut plots summarizing the average frequencies (n = 5 donors) of target killing outcomes in interactions between single NK cells and the indicated number of target cells. Stars represent significance of *P* values ($P_{22}$, $P_{23}$, $P_{24}$), calculated as detailed in supplemental Table 1. F, phenylalanine; nd, not determined; V, valine.

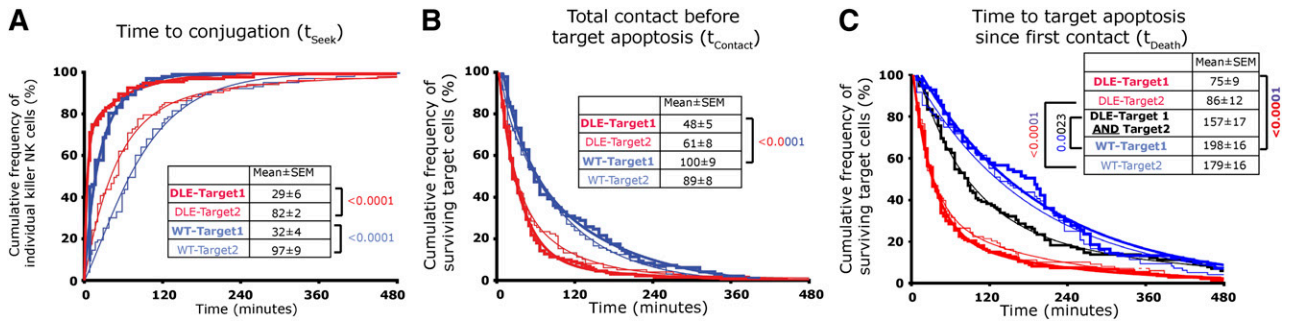


**Figure 4. DLE-HuM195 facilitates serial killing by NK cells by rapidly shortening the kinetics of target apoptosis.** Cumulative association/decay curves (jagged lines) of (A) $t_{Seek}$, (B) $t_{Contact}$, and (C) $t_{Death}$ for each single serial killer NK cell in interaction with multiple targets (2-3 targets). The solid lines represent the best-fit line modeled using either 2-phase or single-phase decay/associations. The parameters obtained from the curve fit are shown in supplemental Table 3. These data are derived from a total of 133 serial killer NK cells interacting with DLE-Targets and 97 serial killer NK cells interacting with wt-Targets. *P* values were calculated for each panel, as listed in supplemental Table 1 ($P_{25}$-$P_{32}$).

hit (75 ± 9 minutes for DLE-HuM195 vs 198 ± 16 minutes for wt-HuM195; $P_{28} < .0001$) were accelerated for DLE-Targets (Figure 4B-C). For all serial killers encountering DLE-Targets or wt-Targets, comparisons of the kinetics between each of the targets encountered by individual NK cells (target 1 vs target 2; Figure 4A-C) showed no differences except for $t_{Seek}$ (*P* values: $P_{29} = .3$, $P_{30} = .4$, and $P_{31} < .0001$). Collectively, these data suggest that the increased serial killing frequency of NK cells when encountering DLE-Targets can be linked to accelerated cytotoxic efficiency; the time taken by the effectors to kill 2 separate DLE-Targets is shorter than the time taken to kill a single wt-Target ($P_{32} = .0023$; Figure 4C; supplemental Videos 3 and 4). Furthermore, the effectors displayed kinetic boosting; conjugation to multiple DLE-Targets presumably enabled integration of signals derived from multiple targets, as $t_{Contact}$ for serial killers (48 ± 5 minutes) before killing the first DLE-Target was significantly lower than the $t_{Contact}$ (78 ± 4 minutes) for cytotoxic NK cells that only encountered a single DLE-Target (Figures 2D and 4B; $P_{33} = .0003$). This advantage was selective only for the interaction with the first target, as the kinetics of killing of the second target were largely the same compared with single targets (Figures 2 and 4).

### DLE-HuM195 improves ADCC and serial killing by freshly ex vivo isolated NK cells

To corroborate the results obtained using the expanded NK cells, the ability of DLE-HuM195 to improve NK cell-mediated ADCC and serial killing was tested using unactivated, ex vivo isolated NK cells. Across 3 separate donor samples, within nanowells containing a single NK cell and 1 to 3 target cells, and after 6 hours of incubation, a mean of 21% (range: 12-31%) of effector NK cells induced apoptosis of DLE-Targets, whereas only a mean of 10% (range: 7-12%) induced apoptosis of wt-Targets ($P_{34} < .0001$; Figure 5A). In the same timeframe, only a mean of 1% (range: 0-2%) of individual NK cells induced target cell apoptosis in the absence of mAb. We also evaluated the ability of these NK cells to participate in serial killing (Figure 5B). As expected, when encountering 2 or 3 DLE-Targets, a mean of 14% (range: 9-23%) of individual NK cells killed at least 2 targets, which was significantly higher than the mean of 3% (range: 3-4%) of effectors killing 2 or more wt-Targets ($P_{35} < .0001$) (Figure 5B). Furthermore, in accordance with results observed for expanded NK cells, AICD displayed donor variation, with only 1 of the 3 samples tested displaying increased AICD on incubation with DLE-targets compared with wt-Targets ($P_{36} = .0006$; supplemental Figure 9). Finally, to test whether the superior cytotoxic and serial killing responses were linked to better NK cell activation, we measured the phosphorylation of ZAP-70, a signaling molecule downstream of the CD16–CD3zeta complex, in ex vivo, nonexpanded, individual cells.[36] As expected, ZAP-70 phosphorylation was induced rapidly when NK cells were cross-linked with DLE-HuM195, whereas no such response was observed when NK cells were cross-linked with wt-HuM195 (Figure 5C; 14% ± 2% for DLE-HuM195 vs 1 ± 1% for wt-HuM195; $P_{37} = .04$). The specificity was confirmed by the near-complete abrogation of the response on preincubation of NK cells with an Fc blocking reagent (2% ± 1%). These results suggest that the ability of DLE-HuM195 to induce rapid activation of NK cells might explain the enhancement in cytotoxic responses.

## Discussion

We implemented TIMING, a high-throughput single-cell assay based on nanowell grids to discern the effect of Fc engineering on the interaction between individual NK cells and mAb-coated tumor cells. At an E:T ratio of exactly 1:1, as anticipated by the increased affinity of engineered Fc for CD16 on NK cells, the overall duration of contact of individual cytotoxic NK cells with DLE-Targets was significantly longer than with wt-Targets (supplemental Figure 6). Consistent with this observation, the $n_{Conjugates}$ required before NK cell-mediated cytotoxicity was lower with the DLE-Targets in comparison with the wt-Targets. The total cumulative duration of contact that resulted in target cell lysis, $t_{Contact}$, however, was unchanged, implying that the net overall contact did not define the kinetics of target cell induction of apoptosis. To the contrary, $t_{Death}$, the time lag between first conjugation and target apoptosis, was faster for NK cells interacting with DLE-Targets in comparison with wt-Targets. Furthermore, at this E:T ratio, both $t_{Contact}$ and $t_{Death}$ were significantly shorter for NK cells interacting with DLE-Targets as compared with K562 cells. Taken together, these results highlight that DLE-HuM195 promotes superior NK cell responses by facilitating efficient activation that led to faster execution of the target cell; this effect is not affected by CD16 158 allotypes.

In addition to single-killer NK cells, serial killer effectors were also profiled. At an E:T ratio of 1:2 to 4, the frequency of NK cells that participated in multiple target hits increased when interacting with DLE-Targets in comparison with wt-Targets (Figure 3). Both

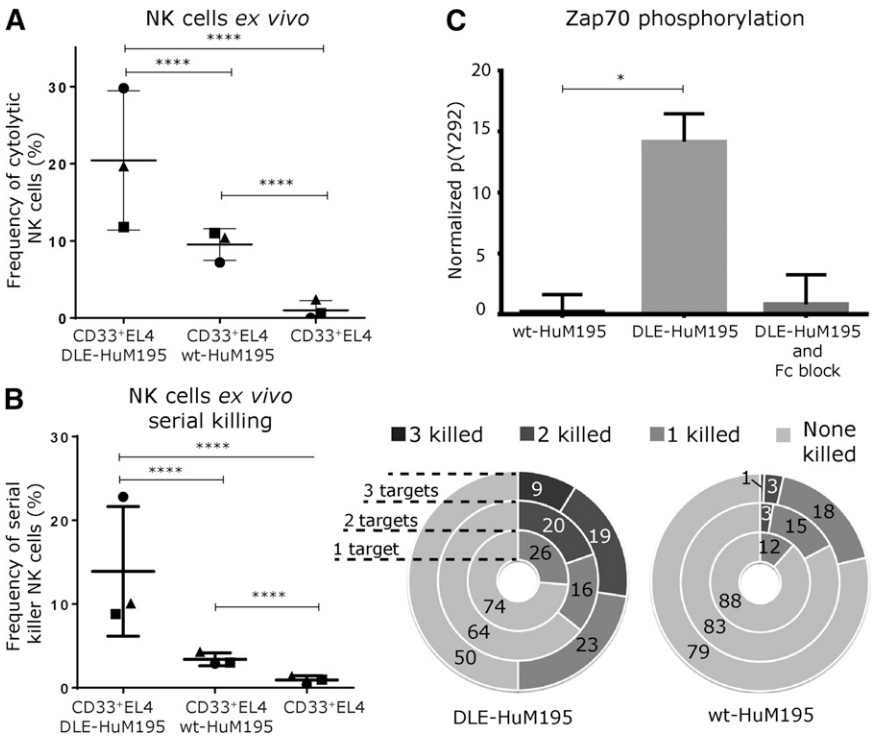


**Figure 5. DLE-HuM195 improves ADCC and serial killing by unactivated NK cells ex vivo and increases CD16-mediated signaling.** The 6-hour single-cell endpoint assay was used to determine (A) the overall frequencies of NK cell-mediated ADCC (at least 2810 events were analyzed for each donor and mAb condition tested), and (B) overall serial killing frequencies (ability to kill at least 2 targets) of NK cells (E:T ratio, 1:2-3) (an average of at least 120 events were analyzed for each donor and mAb condition tested). Donut plots summarizing the frequency of killing outcomes of the interactions between single NK cells and the indicated number of target cells are also shown. Values displayed are background-corrected; bars represent mean ± SD. (C) Normalized ZAP-70 phosphorylation in single NK cells as measured by phospho-flow and expressed as baseline-corrected percentage of maximum, the latter being obtained by cross-linking of CD16. The values are presented as mean ± SD derived from 4 separate donors. Stars represent *P* values for each panel and were calculated as described in supplemental Table 1 ($P_{34}$-$P_{37}$).

$t_{Contact}$ and $t_{Death}$ for individual NK cells to induce apoptosis of DLE-Target cells were substantially lower than with wt-Targets. Integrating $t_{Seek}$ and $t_{Death}$ indicated that when encountering multiple DLE-Targets, individual NK cells were able to efficiently integrate CD16 signaling derived from simultaneous conjugates (supplemental Video 3) to accelerate the kinetics of target cell death. Thus, the total contact time required before DLE-Target cell apoptosis is lower when conjugated to multiple targets in comparison with single targets, displaying kinetic boosting. This finding is consistent with the observation that when incubated with multiple targets, NK-cell cytotoxic events were not independent (supplemental Table 5). This efficiency in eliciting functional responses confers a superior advantage at higher cell densities, and kinetic boosting enabled NK cells to kill 2 separate DLE-Targets within the same timeframe needed to kill a single wt-Target (Figure 4C). Because enhanced activation can also promote NK cell AICD, this parameter was measured as a function of each of the mAbs tested. Unlike ADCC, NK cell AICD displayed donor-specific variation with NK cells from 3 of 5 donors displaying enhanced AICD when interacting with DLE-Targets. The validity of these results was also confirmed with unactivated ex vivo NK cells. Finally, we verified that superior activation, as measured by ZAP-70 phosphorylation, enabled by CD16 on binding of DLE-HuM195, is likely to be responsible for the accrued and accelerated response of NK cells.

With regard to the treatment of AML, recent clinical data have reinvigorated interest in the targeting of CD33, especially as profiling of large panels of primary AML tumors demonstrated that CD33 is expressed on more than 99% of samples.[37] Furthermore, CD33 is expressed on leukemic stem cells from patients with AML at significantly greater levels compared with hematopoietic stem cells isolated from healthy donors.[37] Indeed, targeting of CD33 using either bispecific T-cell engagers, anti-CD33 × anti-CD3, or bispecific killer-cell engagers, anti-CD33 × anti-CD16, has shown preclinical promise.[38,39] As our results with the AML cell lines demonstrate, Fc-engineered DLE-HuM195 may provide an avenue to enhance preclinical, and eventually clinical, efficacy of targeting CD33.

The results outlined here can have important broader implications for immunotherapeutic treatments. First, NK cells express additional receptors that can directly recognize tumor cells, and it has been recently demonstrated using 2-photon microscopy that mAbs can act as molecular bridges to recruit NK cells to malignantly transformed cells by increasing the duration of contact.[40] As we demonstrate, Fc-engineered mAb can also increase NK cell-mediated functional responses. Although negative signals transmitted by tumor cells can dampen NK cell responses, of all the activating receptors found on NK cells, it has been shown that mAb-derived CD16 signaling is the most likely to overcome inhibitory signals.[41,42] Second, preclinical and clinical data using Fc-engineered mAbs have demonstrated a transient decrease in the frequency of circulating NK cells in some patients.[30,43] As our results suggest, this could be a result of induction of AICD in NK cells, and this effect is clearly heterogeneous and donor-dependent. Third, with the ability of newer methods to enable the massive expansion of NK cells ex vivo, adoptive therapy using NK cells is being investigated for the treatment of many different cancers, often in conjunction with mAb therapy.[34,44,45] TIMING, as demonstrated in the current context, provides a framework for quantifying the effector functionality of individual NK cells that make up the inoculum for human application.

## Acknowledgments

This publication was supported by Cancer Prevention Research Institute of Texas Awards RP130570 and RP110553, the National Institutes of Health (R01CA174385), the Welch Foundation (E-1774), and a Melanoma Research Alliance Young Investigator Award (to N.V.), as well as a Scholar Award from the St. Baldrick's

Foundation and a Translational Research Program Award from the Leukemia & Lymphoma Society (to D.A.L.). G.G. would like to acknowledge funding from the Clayton Research Foundation.

## Authorship

Contribution: G.R., V.S., D.A.L., and N.V. designed the study; W.K., W.C., and G.G. were responsible for mAb engineering; G.R., V.S., W.K., I.L., and A. Mahendra acquired the data; N.R.-V., A. Merouane, and B.R. developed the analytical tools for image segmentation and processing; G.R., V.S., D.A.L., and N.V. analyzed and interpreted the data; G.R. and N.V. wrote the manuscript; and V.S., A. Mahendra, G.G., and D.A.L. made critical revisions of the manuscript.

Conflict-of-interest disclosure: The authors declare no competing financial interests.

Correspondence: Dean A. Lee, Division of Pediatrics, Cell Therapy Section, University of Texas M.D. Anderson Cancer Center, Houston, TX 77030; e-mail: dalee@mdanderson.org; and Navin Varadarajan, Department of Chemical and Biomolecular Engineering, University of Houston, Houston, TX 77204; e-mail: nvaradar@central.uh.edu.

## References

1. Weiner LM, Surana R, Wang S. Monoclonal antibodies: versatile platforms for cancer immunotherapy. *Nat Rev Immunol.* 2010;10(5): 317-327.
2. Kellner C, Derer S, Valerius T, Peipp M. Boosting ADCC and CDC activity by Fc engineering and evaluation of antibody effector functions. *Methods.* 2014;65(1):105-113.
3. Stavenhagen JB, Gorlatov S, Tuaillon N, et al. Fc optimization of therapeutic antibodies enhances their ability to kill tumor cells in vitro and controls tumor expansion in vivo via low-affinity activating Fcgamma receptors. *Cancer Res.* 2007;67(18):8882-8890.
4. Jung ST, Reddy ST, Kang TH, et al. Aglycosylated IgG variants expressed in bacteria that selectively bind FcgammaRI potentiate tumor cell killing by monocyte-dendritic cells. *Proc Natl Acad Sci USA.* 2010;107(2):604-609.
5. Zalevsky J, Leung IW, Karki S, et al. The impact of Fc engineering on an anti-CD19 antibody: increased Fcgamma receptor affinity enhances B-cell clearing in nonhuman primates. *Blood.* 2009;113(16):3735-3743.
6. Bowles JA, Wang SY, Link BK, et al. Anti-CD20 monoclonal antibody with enhanced affinity for CD16 activates NK cells at lower concentrations and more effectively than rituximab. *Blood.* 2006; 108(8):2648-2654.
7. Horton HM, Bernett MJ, Peipp M, et al. Fc-engineered anti-CD40 antibody enhances multiple effector functions and exhibits potent in vitro and in vivo antitumor activity against hematologic malignancies. *Blood.* 2010;116(16): 3004-3012.
8. Jung ST, Kelton W, Kang TH, et al. Effective phagocytosis of low Her2 tumor cell lines with engineered, aglycosylated IgG displaying high FcγRIIa affinity and selectivity. *ACS Chem Biol.* 2013;8(2):368-375.
9. Bryceson YT, Chiang SC, Darmanin S, et al. Molecular mechanisms of natural killer cell activation. *J Innate Immun.* 2011;3(3):216-226.
10. Sun JC, Lanier LL. NK cell development, homeostasis and function: parallels with $CD8^+$ T cells. *Nat Rev Immunol.* 2011;11(10): 645-657.
11. Long EO, Kim HS, Liu D, Peterson ME, Rajagopalan S. Controlling natural killer cell responses: integration of signals for activation and inhibition. *Annu Rev Immunol.* 2013;31:227-258.
12. Beum PV, Lindorfer MA, Taylor RP. Within peripheral blood mononuclear cells, antibody-dependent cellular cytotoxicity of rituximab-opsonized Daudi cells is promoted by NK cells and inhibited by monocytes due to shaving. *J Immunol.* 2008;181(4):2916-2924.
13. Grier JT, Forbes LR, Monaco-Shawver L, et al. Human immunodeficiency-causing mutation defines CD16 in spontaneous NK cell cytotoxicity. *J Clin Invest.* 2012;122(10):3769-3780.
14. Clynes RA, Towers TL, Presta LG, Ravetch JV. Inhibitory Fc receptors modulate in vivo cytotoxicity against tumor targets. *Nat Med.* 2000; 6(4):443-446.
15. de Haij S, Jansen JH, Boross P, et al. In vivo cytotoxicity of type I CD20 antibodies critically depends on Fc receptor ITAM signaling. *Cancer Res.* 2010;70(8):3209-3217.
16. Cartron G, Dacheux L, Salles G, et al. Therapeutic activity of humanized anti-CD20 monoclonal antibody and polymorphism in IgG Fc receptor FcgammaRIIIa gene. *Blood.* 2002;99(3): 754-758.
17. Koene HR, Kleijer M, Algra J, Roos D, von dem Borne AE, de Haas M. Fc gammaRIIIa-158V/F polymorphism influences the binding of IgG by natural killer cell Fc gammaRIIIa, independently of the Fc gammaRIIIa-48L/R/H phenotype. *Blood.* 1997;90(3):1109-1114.
18. Weng WK, Levy R. Two immunoglobulin G fragment C receptor polymorphisms independently predict response to rituximab in patients with follicular lymphoma. *J Clin Oncol.* 2003;21(21):3940-3947.
19. Herter S, Birk MC, Klein C, Gerdes C, Umana P, Bacac M. Glycoengineering of therapeutic antibodies enhances monocyte/macrophage-mediated phagocytosis and cytotoxicity. *J Immunol.* 2014;192(5):2252-2260.
20. Walter RB, Appelbaum FR, Estey EH, Bernstein ID. Acute myeloid leukemia stem cells and CD33-targeted immunotherapy. *Blood.* 2012; 119(26):6198-6208.
21. Cowan AJ, Laszlo GS, Estey EH, Walter RB. Antibody-based therapy of acute myeloid leukemia with gemtuzumab ozogamicin. *Front Biosci (Landmark Ed).* 2013;18:1311-1334.
22. Rowe JM, Löwenberg B. Gemtuzumab ozogamicin in acute myeloid leukemia: a remarkable saga about an active drug. *Blood.* 2013;121(24):4838-4841.
23. Caron PC, Co MS, Bull MK, Avdalovic NM, Queen C, Scheinberg DA. Biological and immunological features of humanized M195 (anti-CD33) monoclonal antibodies. *Cancer Res.* 1992;52(24): 6761-6767.
24. Sutherland MK, Yu C, Lewis TS, et al. Anti-leukemic activity of lintuzumab (SGN-33) in preclinical models of acute myeloid leukemia. *MAbs.* 2009;1(5):481-490.
25. Choi PJ, Mitchison TJ. Imaging burst kinetics and spatial coordination during serial killing by single natural killer cells. *Proc Natl Acad Sci USA.* 2013; 110(16):6488-6493.
26. Yamanaka YJ, Berger CT, Sips M, Cheney PC, Alter G, Love JC. Single-cell analysis of the dynamics and functional outcomes of interactions between human natural killer cells and target cells. *Integr Biol (Camb).* 2012;4(10):1175-1184.
27. Liadi I, Roszik J, Romain G, Cooper LJ, Varadarajan N. Quantitative high-throughput single-cell cytotoxicity assay for T cells. *J Vis Exp.* 2013;(72):e50058.
28. Vanherberghen B, Olofsson PE, Forslund E, et al. Classification of human natural killer cells based on migration behavior and cytotoxic response. *Blood.* 2013;121(8):1326-1334.
29. Mazor Y, Keydar I, Benhar I. Humanization and epitope mapping of the H23 anti-MUC1 monoclonal antibody reveals a dual epitope specificity. *Mol Immunol.* 2005;42(1):55-69.
30. Lazar GA, Dang W, Karki S, et al. Engineered antibody Fc variants with enhanced effector function. *Proc Natl Acad Sci USA.* 2006;103(11): 4005-4010.
31. Liu Z, Gunasekaran K, Wang W, et al. Asymmetrical Fc engineering greatly enhances antibody-dependent cellular cytotoxicity (ADCC) effector function and stability of the modified antibodies. *J Biol Chem.* 2014;289(6):3571-3590.
32. Friedrich M, Henn A, Raum T, et al. Preclinical characterization of AMG 330, a CD3/CD33-bispecific T-cell-engaging antibody with potential for treatment of acute myelogenous leukemia. *Mol Cancer Ther.* 2014;13(6):1549-1557.
33. Dunn C, Chalupny NJ, Sutherland CL, et al. Human cytomegalovirus glycoprotein UL16 causes intracellular sequestration of NKG2D ligands, protecting against natural killer cell cytotoxicity. *J Exp Med.* 2003;197(11):1427-1439.
34. Denman CJ, Senyukov VV, Somanchi SS, et al. Membrane-bound IL-21 promotes sustained ex vivo proliferation of human natural killer cells. *PLoS ONE.* 2012;7(1):e30264.
35. Somanchi SS, Senyukov VV, Denman CJ, Lee DA. Expansion, purification, and functional assessment of human peripheral blood NK cells. *J Vis Exp.* 2011;(48): 2540.
36. Lichtfuss GF, Meehan AC, Cheng WJ, et al. HIV inhibits early signal transduction events triggered by CD16 cross-linking on NK cells, which are important for antibody-dependent cellular cytotoxicity. *J Leukoc Biol.* 2011;89(1):149-158.
37. Krupka C, Kufer P, Kischel R, et al. CD33 target validation and sustained depletion of AML blasts in long-term cultures by the bispecific T-cell-engaging antibody AMG 330. *Blood.* 2014;123(3): 356-365.
38. Laszlo GS, Gudgeon CJ, Harrington KH, et al. Cellular determinants for preclinical activity of a novel CD33/CD3 bispecific T-cell engager (BiTE) antibody, AMG 330, against human AML. *Blood.* 2014;123(4):554-561.
39. Wiernik A, Foley B, Zhang B, et al. Targeting natural killer cells to acute myeloid leukemia in vitro with a CD16 x 33 bispecific killer cell engager

and ADAM17 inhibition. *Clin Cancer Res.* 2013; 19(14):3844-3855.

40. Deguine J, Breart B, Lemaître F, Bousso P. Cutting edge: tumor-targeting antibodies enhance NKG2D-mediated NK cell cytotoxicity by stabilizing NK cell-tumor cell interactions. *J Immunol.* 2012;189(12):5493-5497.
41. Chan WK, Kung Sutherland M, Li Y, Zalevsky J, Schell S, Leung W. Antibody-dependent cell-mediated cytotoxicity overcomes NK cell resistance in MLL-rearranged leukemia expressing inhibitory KIR ligands but not activating ligands. *Clin Cancer Res.* 2012;18(22): 6296-6305.
42. Bryceson YT, Ljunggren HG, Long EO. Minimal requirement for induction of natural cytotoxicity and intersection of activation signals by inhibitory receptors. *Blood.* 2009;114(13):2657-2666.
43. Veeramani S, Wang SY, Dahle C, et al. Rituximab infusion induces NK activation in lymphoma patients with the high-affinity CD16 polymorphism. *Blood.* 2011;118(12):3347-3349.
44. Ni J, Miller M, Stojanovic A, Garbi N, Cerwenka A. Sustained effector function of IL-12/15/18-preactivated NK cells against established tumors. *J Exp Med.* 2012;209(13):2351-2365.
45. Cheng M, Chen Y, Xiao W, Sun R, Tian Z. NK cell-based immunotherapy for malignant diseases. *Cell Mol Immunol.* 2013;10(3): 230-252.